

Atomic structure of the metastable $c(4 \times 4)$ reconstruction of Si(100)

R. I. G. Uhrberg,* John E. Northrup, D. K. Biegelsen, R. D. Bringans, and L.-E. Swartz
Xerox Corporation, Palo Alto Research Center, Palo Alto, California 94304

(Received 19 May 1992)

A $c(4 \times 4)$ reconstruction can be formed on the clean Si(100) surface by special surface treatment techniques. We have studied the atomic structure of this metastable phase, which is prepared by hydrogen exposure and annealing, using scanning tunneling microscopy and first-principles total-energy calculations. A new model is derived which has two types of surface dimers oriented parallel and perpendicular to the underlying 2×1 dimer rows. Our results are thus in disagreement with the missing dimer model which has earlier been proposed in the literature.

The atomic structure of the clean Si(100) surface has been the subject of many studies using a large number of different characterization techniques. So far the main effort has been concentrated on the 2×1 room-temperature phase and the $c(4 \times 2)$ phase obtained at low temperatures. It is now well established that these reconstructions of the Si(100) surface are due to dimerization of the atoms in the first layer. Beside these well-known and extensively studied reconstructions a $c(4 \times 4)$ reconstruction has been repeatedly reported in the literature for the clean Si(100) surface.¹⁻⁸ The four different techniques that have been used to obtain the $c(4 \times 4)$ surface have one thing in common, i.e., the temperatures at which the $c(4 \times 4)$ phase forms are confined to a rather limited interval which is usually reported to be ≈ 600 – 700 °C. The earliest report of a $c(4 \times 4)$ reconstruction is due to Thomas and Francombe.¹ These authors grew Si on Si(100) and found that a $c(4 \times 4)$ reconstruction appeared when the growth temperature was between 650 and 700 °C. A $c(4 \times 4)$ reconstruction was also observed by Sakamoto *et al.*² during Si growth. The temperature interval reported by those authors was, however, higher (700–800 °C). A second way of preparing the $c(4 \times 4)$ surface was reported by Wang, Lin, and Wang,⁴ who prepared the surface by cooling the sample from 1100 °C and keeping it at 600 °C for 5 min. A third preparation procedure has been presented by Kato *et al.*,⁵ which involves hydrogen exposure followed by annealing at temperatures between 570 and 690 °C. Finally, the $c(4 \times 4)$ reconstruction was recently observed during growth on Si(100) at temperatures between 645 and 775 °C using a disilane gas source.^{6,7}

In some of the earlier studies⁴⁻⁷ it has been proposed that the $c(4 \times 4)$ reconstruction is due to an ordering of missing dimer defects. The simplest way of obtaining a $c(4 \times 4)$ periodicity would be to place one missing dimer defect at each corner of the $c(4 \times 4)$ primitive cell. However, in a recent scanning tunneling microscopy (STM) study by Ide and Mizutani⁸ of the $c(4 \times 4)$ surface it was shown that the images were inconsistent with the simple missing dimer model. The filled and empty state images were instead interpreted in terms of a single Si dimer per $c(4 \times 4)$ primitive cell forming the reconstruction. No information about the atomic structure between these di-

mers could, however, be derived in that STM study.⁸

The STM results presented in this paper confirm the basic results of Ref. 8, i.e., the existence of Si dimers arranged in a $c(4 \times 4)$ pattern and that the STM images are inconsistent with the simple missing dimer model. Based on our more detailed STM results and first-principles total-energy calculations we present a new model for the $c(4 \times 4)$ surface which shows similarities with the 2×2 parallel ad-dimer model recently established for Al, Ga, and In overlayers on Si(100).⁹ A transformation is achieved from the basic 2×2 periodicity of parallel ad-dimers, to a $c(4 \times 4)$ periodicity by breaking 50% of the dimer bonds in the underlying 2×1 rows in an ordered way and inserting dimers oriented perpendicular to the 2×1 dimers. This results in the structure we refer to as

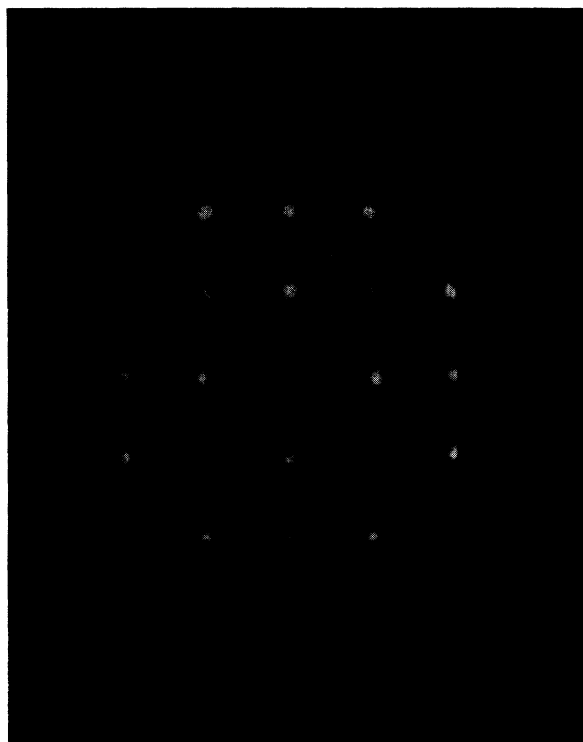


FIG. 1. Low-energy electron-diffraction pattern from the Si(100) $c(4 \times 4)$ surface. The primary beam energy was 58.0 eV.

the mixed ad-dimer structure having both parallel and perpendicular ad-dimers.

The Si(100) samples used in this study were of two types, i.e., As-doped ($\approx 5 \text{ m}\Omega \text{ cm}$) and P-doped ($\approx 10 \text{ m}\Omega \text{ cm}$). The As-doped samples were cleaned *ex situ* according to the method by Ishizaka and Shiraki.¹⁰ The P-doped samples were submerged in a 1:1 solution of H_2SO_4 and H_2O_2 for 10 min. After rinsing in deionized water they were dipped in HF for 30 sec and rinsed again. Finally, the P-doped samples were cleaned in an ozone-cleaner for about 2 min. After insertion into the experi-

mental system, which has been described elsewhere,¹¹ the samples were outgassed for several hours at 600°C . After the final annealing [a few minutes at 930°C (As doped) or 1030°C (P doped)] the clean Si(100) 2×1 surfaces were characterized by low-energy electron diffraction (LEED), x-ray photoelectron spectroscopy (XPS), and STM. In order to obtain the $c(4\times 4)$ reconstruction the samples were typically exposed to 20 000 L ($1 \text{ L} = 10^{-6} \text{ Torr sec}$) of hydrogen in the presence of a hot ($\approx 1700^\circ\text{C}$) tungsten filament. After the exposure, the surfaces exhibited a 1×1 LEED pattern. The samples were then annealed at

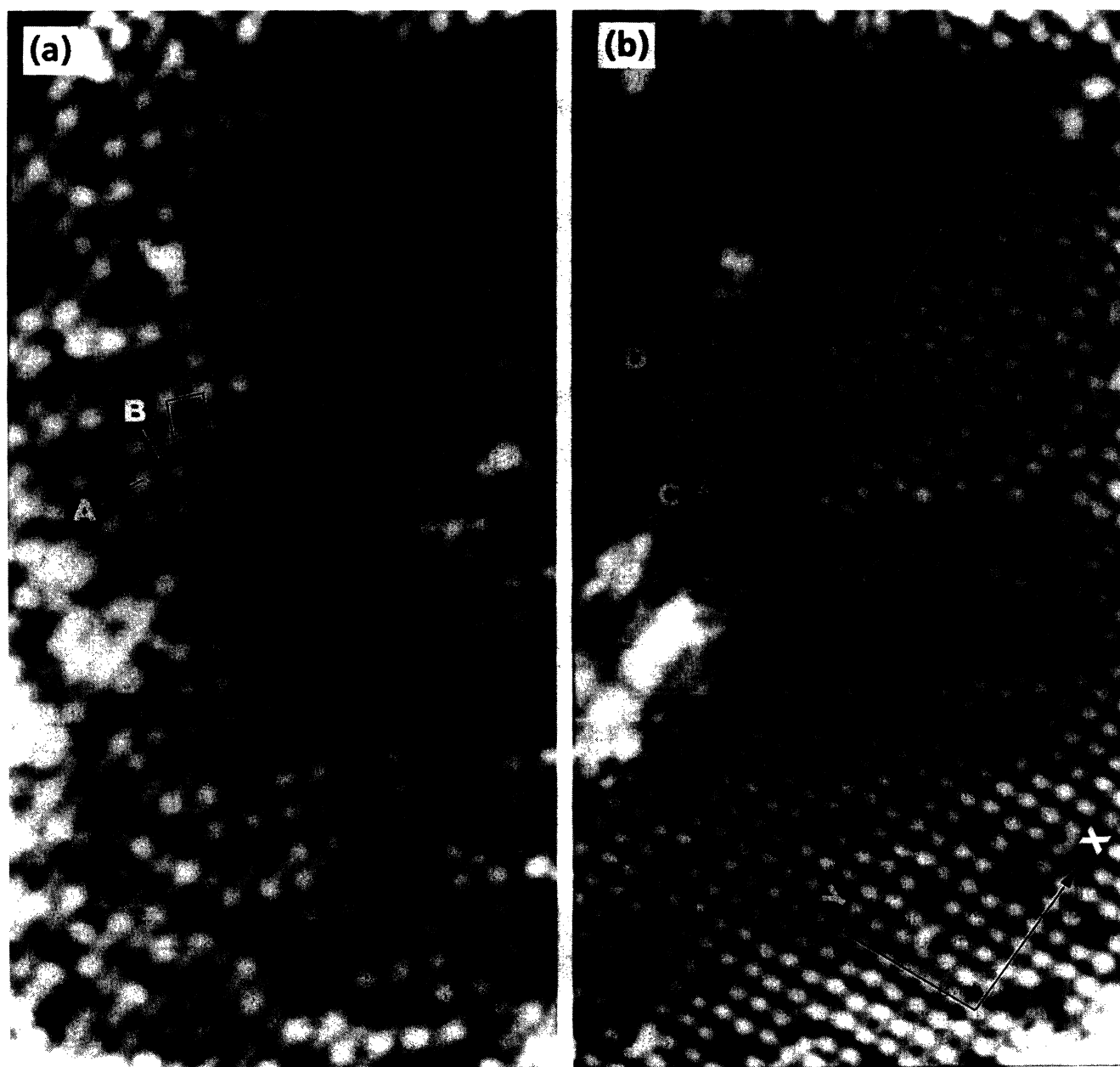


FIG. 2. (a) Filled state image of the Si(100) $c(4\times 4)$ surface ($\approx 160\times 320 \text{ \AA}^2$) obtained for a sample bias V_s of -1.5 V . (b) Simultaneously acquired empty state image of the same area as in (a) for $V_s = 1.5 \text{ V}$. Typical features (A–D) are indicated in the figures. A primitive cell of the $c(4\times 4)$ periodicity ($2\sqrt{2}\times 2\sqrt{2}\text{-}R45^\circ$) is shown in the upper parts of the images. The arrows show a section of a row where features A and C are missing.

increasing temperatures while the LEED pattern was inspected. The initial 1×1 pattern caused by the hydrogen exposure changed to a 2×1 pattern at temperatures around $500\text{--}550^\circ\text{C}$. At $\approx 600^\circ\text{C}$ LEED spots of the $(\frac{1}{2}, \frac{1}{2})$ type started to appear. At this stage the LEED pattern thus shows a 2×2 periodicity. Further annealing gave rise to LEED spots of the $(\frac{1}{4}, \frac{1}{4})$ type which are part of the $c(4\times 4)$ pattern (see Fig. 1). The $c(4\times 4)$ surface, once formed, was stable up to $\approx 730^\circ\text{C}$. Above this temperature it transformed irreversibly to the 2×1 reconstruction. The formation temperature of the $c(4\times 4)$ structure is significantly higher than the desorption temperature for hydrogen from Si(100) as discussed in Ref. 5. This together with the fact that the $c(4\times 4)$ surface can be obtained by Si growth on Si(100) (Refs. 1 and 2) implies that the $c(4\times 4)$ surface is free from hydrogen. Further, Auger-electron spectroscopy studies³⁻⁵ verify that the $c(4\times 4)$ reconstruction corresponds to a contamination-free surface. The results for the atomic structure of the $c(4\times 4)$ surface presented below are based on STM images obtained on seven different samples (both P and As doped). The STM images of the Si(100) $c(4\times 4)$ surface shown in this paper are raw data obtained with a tunneling current of 100 pA. No compensation has been made for thermal drift or systematic skew of the images. Sample biases V_s in the ranges 0.9 to 1.7 and -0.9 to -2.0 V were employed to image the surface.

Figure 2 shows a dual-bias STM image of the Si(100) $c(4\times 4)$ surface. The left part shows the occupied states and the right part the empty states at the same location for a sample bias $V_s = -1.5$ V and $V_s = 1.5$ V, respectively. The typical features observed in the two images are labeled *A*–*D*. The empty state image, Fig. 2(b), is the least complicated and we will start by describing it. The image is dominated by a “square” array of white protrusions which, at first glance, seem to be ordered in a 2×2 pattern by comparing to the small 2×1 area at the mid left part of the image. This appearance of the empty states is very similar to what has been observed for Si(100) 2×2 :Al.¹² However, by comparing the location of the protrusions along the two perpendicular directions *x* and *y*, we find that the pattern does not have a simple 2×2 periodicity. In the *x* direction the white features form a straight chain while they form a zig-zag chain along the *y* direction. The distance between two neighboring features along *x* thus alternates between a “short” and a “long” distance. This modification of the apparent 2×2 structure results in a $c(4\times 4)$ periodicity. The two closely spaced protrusions inside the $c(4\times 4)$ cell are labeled *D*. A second type of feature (*C*) is observed in the STM images at positions corresponding to the corners of the primitive cell. The feature *C* is quite weak in Fig. 2(b). In Fig. 3(b) we show a close-up image of the empty states where *C* is clearly seen. It consists of two closely spaced oblong protrusions.

The images of the occupied states look quite different [see Figs. 2(a) and 3(a)]. Two kinds of features dominate these images. There are bright features (*A*) which locally form a square pattern showing the $c(4\times 4)$ periodicity. The $c(4\times 4)$ unit cell outlined in the unoccupied states

image in Fig. 2(b) is reproduced in the image of the occupied states for comparison. The bright spots *A* are located at the corners of this primitive cell which is the same position as for feature *C* in the unoccupied state image. Between two bright spots in the *x* direction there is a closely spaced pair of protrusions (*B*) which appear less bright in the image. The feature *B* is most evident in the regions where feature *A* is missing (e.g., between the arrows in Fig. 2). Due to pairing the features *B* also form a $c(4\times 4)$ pattern. The position of *B* coincides with the position of *D* in the image of the unoccupied states.

In Fig. 4 we have schematically drawn the appearance of the filled and empty state images. Feature *A* on the occupied side splits into two protrusions labeled *C* for the unoccupied states. In contrast, *B* and *D* show just a small difference between the filled and empty state images. The dumbbell-shaped feature *B* in the filled state image splits into two “circular” ones in the empty state image. This difference is very clear in Fig. 2. The appearance of the different features varies, however, somewhat depending

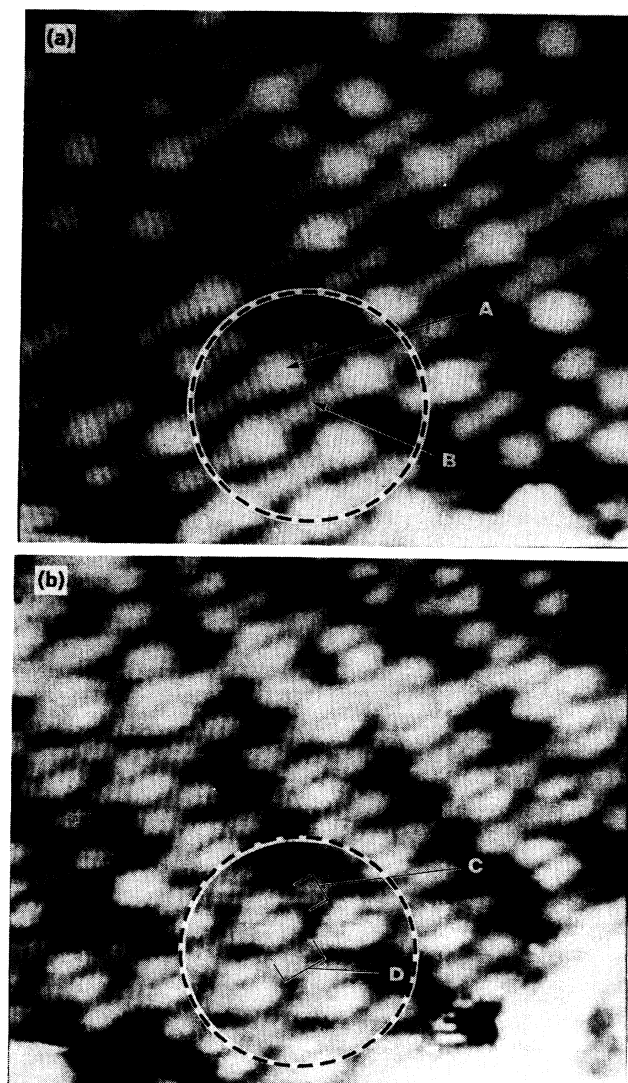


FIG. 3. Same as Fig. 2 but for a smaller area ($\approx 75\times 75 \text{ \AA}^2$). A unit cell of the $c(4\times 4)$ reconstruction is shown inside the circle.

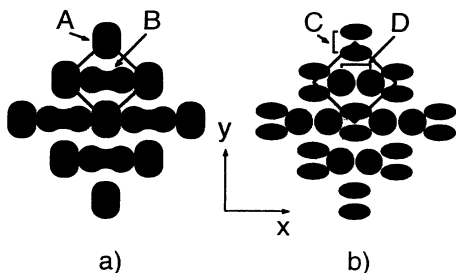


FIG. 4. Schematic drawing of the typical STM features ($A-D$) observed for filled (a) and empty states (b).

on the experimental conditions. In Fig. 3, for instance, we find a much smaller difference between features B and D . Although some variations are observed, the schematic drawings in Fig. 4 summarize what we have observed for the seven samples investigated.

As can be seen from Fig. 2, the STM images of the $c(4\times 4)$ reconstruction are dominated by features B and D . The number of missing protrusions of type B and D in the images is generally much less than is observed for A and C . In Fig. 2 about 13% of the protrusions corresponding to B or D are missing while the number for A or C is as high as 45%. This difference in defect density suggests that the structural elements corresponding to B and D are more basic to the $c(4\times 4)$ reconstruction than those corresponding to A and C . Further, the appearance of the empty state image in Fig. 2(b) indicates that the $c(4\times 4)$ reconstruction may be obtained by modifying a more fundamental 2×2 reconstruction.

Total energy and electronic structure calculations were performed for several possible $c(4\times 4)$ structures. Three $c(4\times 4)$ structures were analyzed: the missing dimer model, the parallel ad-dimer model, and the mixed ad-dimer model. These structures are shown in Fig. 5. In these calculations we employed the first-principles pseudopotential method¹³ and the local-density approximation.¹⁴ The electronic wave functions were expanded in a basis set consisting of plane waves having kinetic energies less than 8 Ry. The summations over the Brillouin zones included two special k points in the irreducible Brillouin zone. A centrosymmetric supercell containing 12 Si layers was employed and forces were used to determine the atomic coordinates for each atom in the supercell except for the atoms in the innermost two layers, which were kept at the bulk positions. The calculated total energies are shown in Table I. These energies are in agreement with experiment in the sense that all three $c(4\times 4)$ structures are higher in energy than the 2×1 buckled dimer structure. It is notable that although these structures have very different dangling-bond densities, their surface energies are equal to within ≈ 0.1 eV per 1×1 cell.

The missing dimer model [Fig. 5(a)] has a lower surface energy than any of the other $c(4\times 4)$ structures but is still 0.37 eV per $c(4\times 4)$ cell higher than the 2×1 buckled dimer. This result may be compared with the calculations reported by Roberts and Needs.¹⁵ They found that a 2×4 missing dimer model was 0.28 eV per 2×4 cell higher than the 2×1 symmetric dimer model. The structural parameters obtained for the missing dimer model in the two calculations are very similar. Here we find bond lengths of 2.19 and 2.21 Å for the surface dimers and 2.72 Å for the strained subsurface dimers.

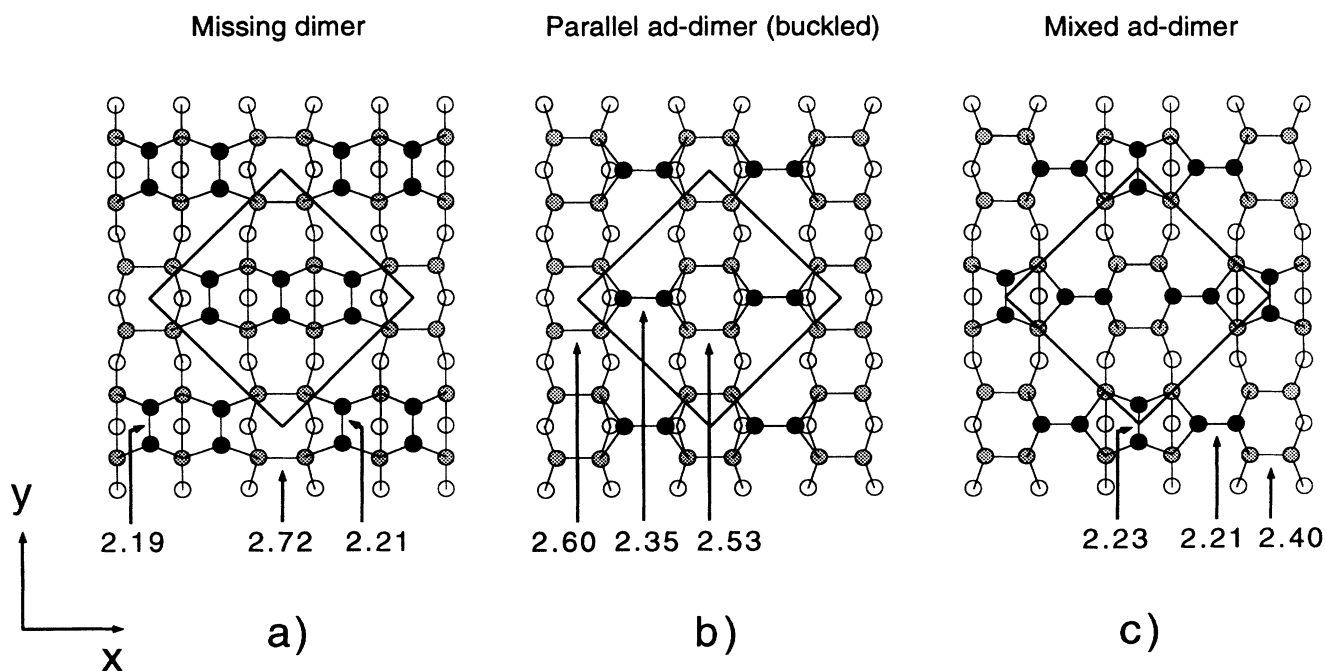


FIG. 5. Schematic models with $c(4\times 4)$ periodicity: (a) Missing dimer model. (b) Parallel ad-dimer model. (c) Mixed ad-dimer model. Solid circles are used to highlight the surface atoms. The square outlines a $c(4\times 4)$ primitive cell. The bond lengths, in Å, were obtained from a total-energy calculation described in the text.

TABLE I. Energies of three $c(4\times 4)$ structures relative to the 2×1 buckled dimer model. Energies are given in eV per 1×1 cell.

Structure	Energy	Dangling-bond density
2×1 buckled dimer	0.0	1
Missing dimer	0.04	0.75
Parallel ad-dimer (buckled)	0.09	0.50
Mixed ad-dimer	0.11	0.75

Roberts and Needs¹⁵ reported 2.19 Å for the surface dimers and 2.71 Å for the subsurface dimers. The reduced dangling-bond density for the missing dimer model is offset by the strain induced in the subsurface dimers, which are strained by 0.37 Å.

The parallel ad-dimer model shown in Fig. 5(b) originated from studies of the bonding of the group-III atoms Al, Ga, and In to the Si(100) surface.⁹ Our calculations indicate that the Si ad-dimer structure is less than 0.1 eV per 1×1 cell higher in energy than the buckled dimer model. For Si ad-dimers, the π states are filled while the π^* states are empty, and a buckling relaxation of the parallel dimers (0.4 Å) gives rise to charge transfer from the down atom to the up atom. This relaxation reduces the symmetry from 2×2 to $c(4\times 4)$. The subsurface dimers, which have bond lengths of 2.53 and 2.60 Å, are highly strained.

The mixed ad-dimer model, illustrated in Fig. 5(c), is obtained by adding one perpendicular ad-dimer to each unit cell of the parallel ad-dimer structure. The addition of the perpendicular dimers releases some of the anisotropic strain in the subsurface dimers, which now exhibit bond lengths of 2.40 Å. The total-energy calculations indicate that this structure is very close in energy to the parallel ad-dimer model. It is possible that a 50-50 mixture of the parallel ad-dimer and mixed ad-dimer structures could have a lower energy than either of the two pure structures.

The STM images are consistent with the mixed ad-dimer structure, but with many of the perpendicular ad-dimers absent. The perpendicular dimers correspond to features *A* and *C* in Figs. 2, 3, and 4. These dimers are symmetric and we thus expect them to give rise to a bean-shaped feature in the filled state image and to two separated maxima for the empty states,¹⁶ which is in good agreement with the STM results. The parallel (buckled) dimers are displaced parallel to the *x* direction. As a consequence the parallel dimers form a zig-zag chain along the *y* direction which corresponds to the zig-zag structure observed for feature *D* and the pairing observed for feature *B*. The occupied and empty state electron densities for the mixed ad-dimer model are shown in Fig. 6. Each of the features of the STM data can be explained in terms of the occupied π states or empty π^* states of the parallel and perpendicular dimers.

It is likely that the preparation conditions which produce the $c(4\times 4)$ structure act to “freeze in” an average atom density which is too low to allow formation of a locally complete layer of the 2×1 dimer structure. If the surface atom density were just a few percent less than a full monolayer the deficiency could be accommodated

easily by creating missing dimer defects in the 2×1 structure. Indeed it has been suggested that the minimum energy state of the Si(100) surface consists of an ordered array of missing dimers,¹⁷ but with a maximum deficit in the surface atom density less than 25%.¹⁵ Here we conjecture that for larger deficits, between 25% and 50%, it becomes energetically unfavorable to accommodate the deficit simply by incorporating missing dimer defects. Instead the surface exhibits a structure having both parallel and perpendicular ad-dimers. We know that the $c(4\times 4)$ structure is a metastable structure which results from special preparation techniques and is observed to be highly defective. Given the metastability two of the experi-

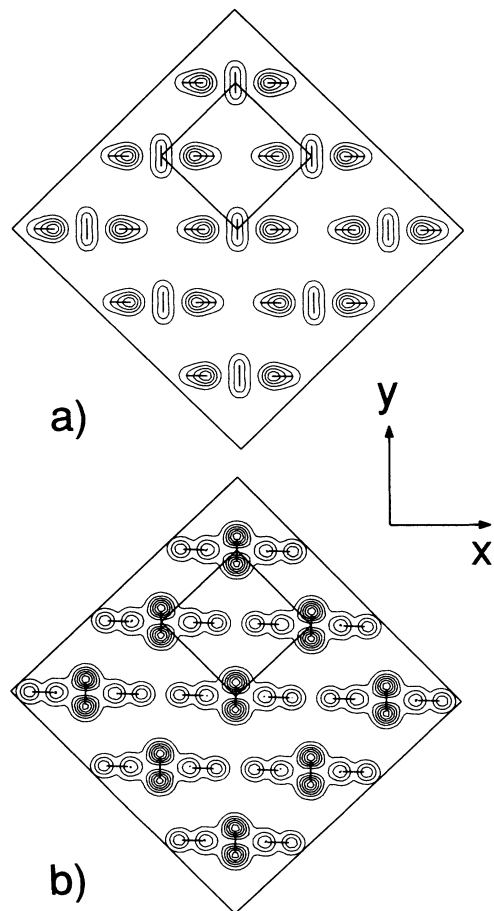


FIG. 6. Contour plot of electron densities in a plane approximately 2 Å above the surface. (a) Plot of occupied states with energies within ≈ 1 eV of E_F . (b) Plot of empty states with energies within ≈ 1 eV of E_F .

mental observations need to be understood. First is that long-range order seems to occur despite a necessarily shorter range adatom diffusion length, and second is that adatom density fluctuations are easily accommodated. The latter point follows from the near equality of energies for various ad-dimer structures. The long range of the $c(4 \times 4)$ symmetric regions presumably follows the long

range of the strain field associated with surface dimerization.

Travel support from the Swedish Natural Science Research Council is gratefully acknowledged (R.I.G.U.). J.E.N. is supported in part by the U.S. ONR Contract No. N00014-92-C-0009.

*Permanent address: Department of Physics and Measurement Technology, Linköping Institute of Technology, S-581 83 Linköping, Sweden.

¹R. N. Thomas and M. H. Francombe, *Appl. Phys. Lett.* **11**, 108 (1967).

²T. Sakamoto, T. Takahashi, E. Suzuki, A. Shoji, H. Kawanami, Y. Komiya, and Y. Tarui, *Surf. Sci.* **86**, 102 (1979).

³K. Müller, E. Lang, L. Hammer, W. Grimm, P. Heilmann, and K. Heinz, in *Determination of Surface Structure by LEED*, edited by P. M. Marcus and F. Jona (Plenum, New York, 1984), p. 483.

⁴H.-C. Wang, R.-F. Lin, and X. Wang, *Phys. Rev. B* **36**, 7712 (1987).

⁵K. Kato, T. Ide, T. Nishimori, and T. Ichinokawa, *Surf. Sci.* **207**, 177 (1988).

⁶S. M. Mokler, W. K. Liu, N. Ohtani, and B. A. Joyce, *Appl. Phys. Lett.* **59**, 1 (1991).

⁷W. K. Liu, S. M. Mokler, N. Ohtani, C. Roberts, and B. A. Joyce, *Surf. Sci.* **264**, 301 (1992).

⁸T. Ide and T. Mizutani, *Phys. Rev. B* **45**, 1447 (1992).

⁹J. E. Northrup, M. C. Schabel, C. J. Karlsson, and R. I. G. Uhrberg, *Phys. Rev. B* **44**, 13 799 (1991).

¹⁰A. Ishizaka and Y. Shiraki, *J. Electrochem. Soc.* **133**, 666 (1986).

¹¹D. K. Biegelsen, R. D. Bringans, J. E. Northrup, and L.-E. Swartz, *Phys. Rev. B* **41**, 5701 (1990).

¹²J. Nogami, A. A. Baski, and C. F. Quate, *Phys. Rev. B* **44**, 1415 (1991).

¹³M. T. Yin and M. L. Cohen, *Phys. Rev. B* **26**, 5668 (1982).

¹⁴W. Kohn and L. Sham, *Phys. Rev.* **140**, A1135 (1965).

¹⁵N. Roberts and R. J. Needs, *J. Phys. Condens. Matter* **1**, 3139 (1989).

¹⁶R. J. Hamers, Ph. Avouris, and F. Bozso, *Phys. Rev. Lett.* **59**, 2071 (1987).

¹⁷K. C. Pandey, in *Proceedings of the Seventeenth International Conference on the Physics of Semiconductors*, edited by D. J. Chadi and W. A. Harrison (Springer-Verlag, New York, 1985), p. 55.

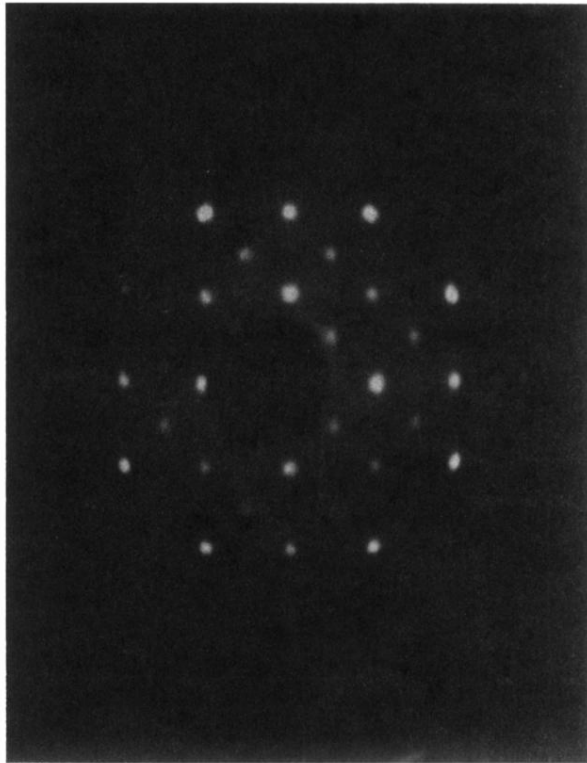


FIG. 1. Low-energy electron-diffraction pattern from the Si(100) $c(4 \times 4)$ surface. The primary beam energy was 58.0 eV.

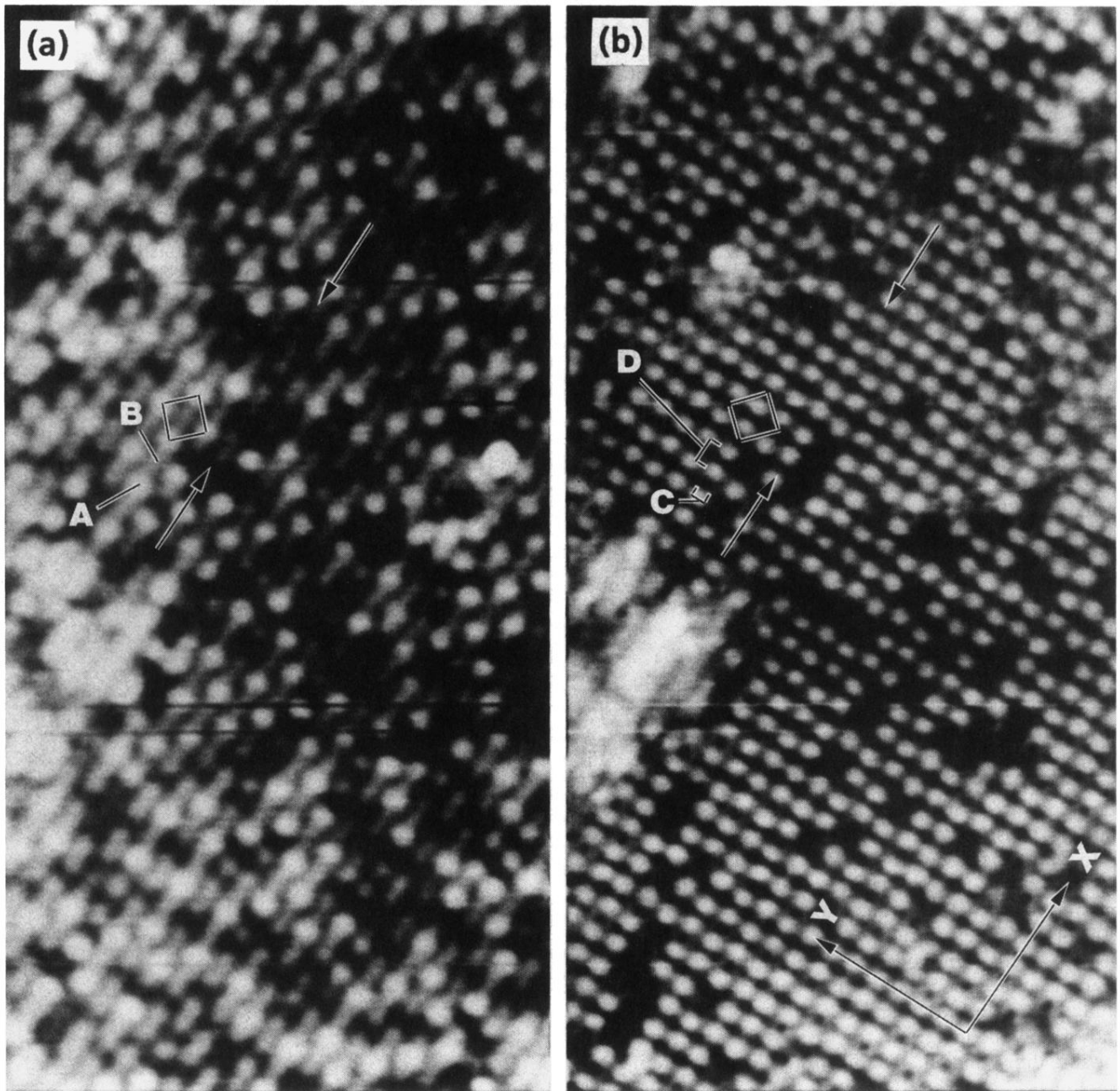


FIG. 2. (a) Filled state image of the Si(100) $c(4\times 4)$ surface ($\approx 160\times 320 \text{ \AA}^2$) obtained for a sample bias V_s of -1.5 V . (b) Simultaneously acquired empty state image of the same area as in (a) for $V_s = 1.5 \text{ V}$. Typical features ($A-D$) are indicated in the figures. A primitive cell of the $c(4\times 4)$ periodicity ($2\sqrt{2}\times 2\sqrt{2}-R45^\circ$) is shown in the upper parts of the images. The arrows show a section of a row where features A and C are missing.

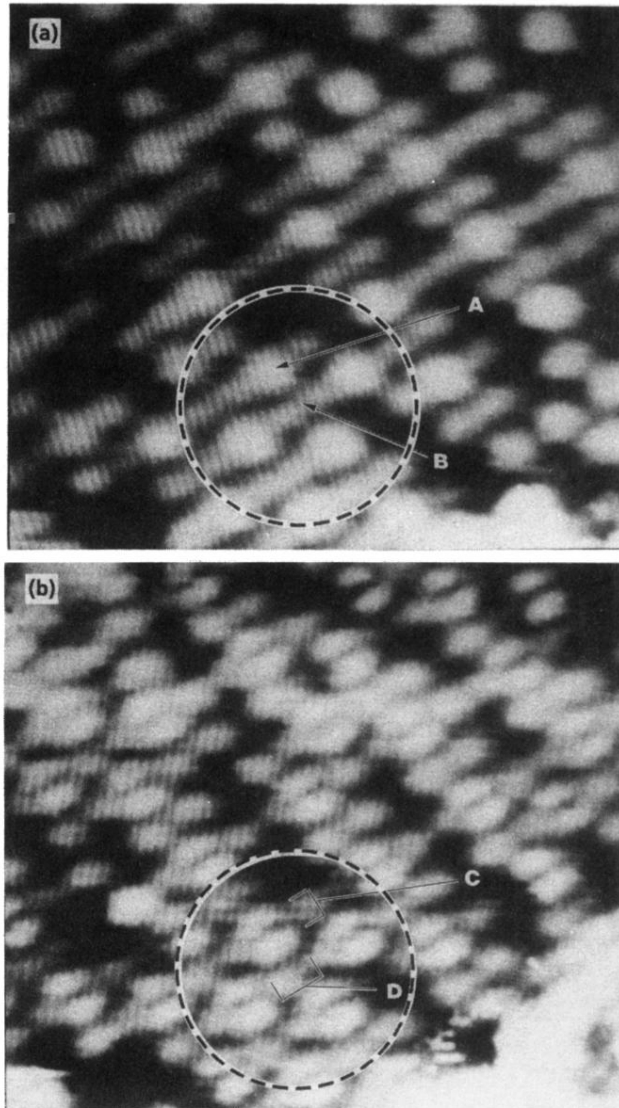
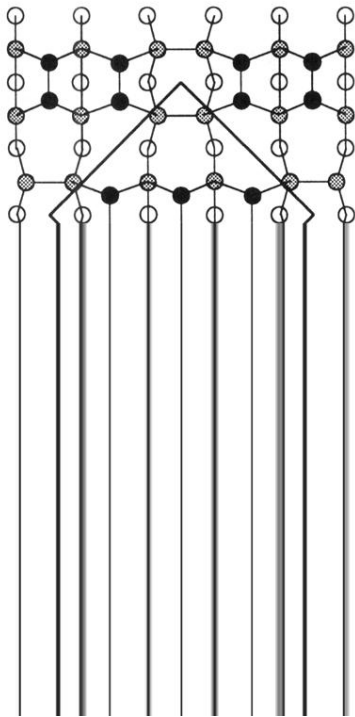
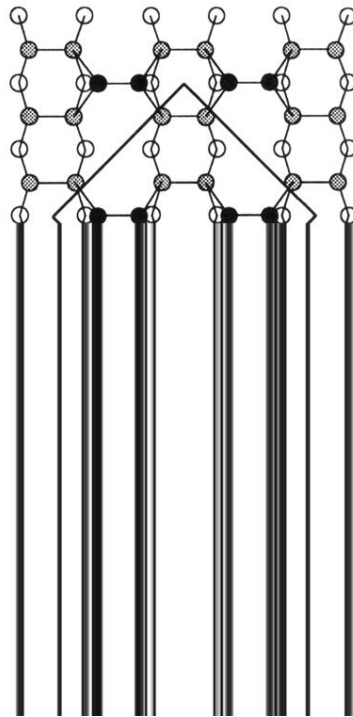


FIG. 3. Same as Fig. 2 but for a smaller area ($\approx 75 \times 75 \text{ \AA}^2$). A unit cell of the $c(4 \times 4)$ reconstruction is shown inside the circle.

Missing dimer



Parallel ad-dimer (buckled)



Mixed ad-dimer

